P12.5 CHARACTERISTICS OF EASTERN AUSTRALIAN-WESTERN TASMAN SEA ENHANCED-Vs AND THEIR CONNECTION TO SEVERE WEATHER

Geoffrey Feren *
Bureau of Meteorology, Melbourne, Victoria, Australia

1. INTRODUCTION

McCann (1983) was the first researcher to use the term "enhanced-V" to describe a thunderstorm cloud top signature observed in enhanced IR GOES imagery that was found to have a strong relationship with U.S. severe weather occurrences. He found that nearly 70% of the 884 April-July 1979 storms characterized by this feature were associated with severe weather, with a median lead-time of about 30 minutes from the first appearance of the enhanced-V to the initial severe weather report.

This and other related papers (e.g. Schlesinger 1984, Adler and Mack 1986, Heymsfield and Blackmer 1988) referred to three main components of the enhanced-V:

(1) A small region of lowest equivalent blackbody temperatures (BTs) resulting from the adiabatic expansion of air parcels associated with an overshooting storm updraft that penetrated the tropopause;

(2) A typically V-shaped region of low BTs, with the storm top usually located near the V's apex point. The "cold V" was generated as strong near tropopause-level winds were diverted around the overshooting top, and additionally eroded the updraft summit, resulting in the downstream transport of cold cloud debris; and

(3) A close-in warm area (CWA), or warm wake, which was enclosed by the V feature, and was generally aligned downwind (with respect to the storm relative flow) from the storm top, thus forming a cold-warm (thermal) couplet. Several theories have been proposed to explain the development of the warm wake, although most commonly it has been attributed to subsidence downwind of the updraft core.

The primary source of satellite data for the initial enhanced-V studies comprised 11 μm IR GOES imagery. However, these studies were limited in the extent to which they could properly isolate and quantify the enhanced-V components, largely because of the relatively low spatial resolution of the imagery (i.e. 8 km at the sub-satellite point, and degrading to about 10 km at mid-latitudes). In particular, Adler et al. (1983) found that the GOES IR observations overestimated the lowest thunderstorm top BTs by as much as 15 K for a mature storm, and noted that a satellite field of view of 1 km would largely eliminate this problem.

Accordingly, Brunner et al. 2006, and Brunner et al. 2007 (hereafter B06 and B07, respectively) used 1 km resolution NOAA Advanced Very High Resolution Radiometer (AVHRR) and NASA Moderate Resolution Imaging Spectroradiometer (MODIS) color-enhanced IR satellite imagery to examine six quantitative enhanced-V parameters and their relationship with U.S. severe weather occurrences. These parameters included (1) TMIN – the coldest point of the V (corresponding to the storm top); (2) TMAX – the highest temperature associated with the CWA; (3) TDIFF and (4) DIST – respectively, the temperature difference and distance between TMIN and TMAX, which form the cold-warm couplet; and (5) DISTARMS and (6) ANGLEARMS – respectively, the average length of, and the angle between the two V arms. Values of all of these parameters are shown for the eastern Australian enhanced-V example displayed in Fig.1. B06 and B07 additionally investigated the relationship

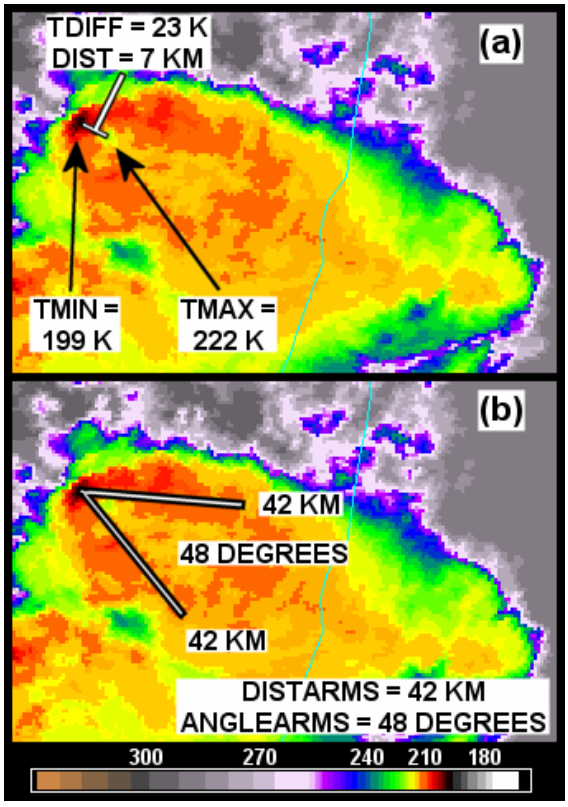

Fig. 1: Enhanced 10.8 μm IR *NOAA-16* image valid 0525 UTC 24 October 2005, showing an eastern Australian example of an enhanced-V. The six enhanced-V quantitative parameters examined by B06/B07 for their relationship to severe weather occurrences included (a) TMIN (K), TMAX (K), TDIFF (K), and DIST (km); and (b) DISTARMS (km) and ANGLEARMS (°).

* *Corresponding author address:* Geoffrey Feren, Victorian Regional Office, Bureau of Meteorology, PO Box 1636, Melbourne, Victoria, 3001, Australia;
e-mail: G.Feren@bom.gov.au

between severe weather and a 7th parameter – i.e. the tropopause-level wind strength (UL WIND SPD) in the vicinity of the enhanced-V.

From their analysis of 450 enhanced-V signatures encompassing approximately four warm season months during 2003 and 2004, B06 identified 11 enhanced-V types that were found to have a high probability of being associated with a tornado and/or large hail (i.e. ≥ 2 cm diameter). Each enhanced-V type required threshold values of two of the quantitative parameters to be satisfied. These are listed in Table 1. They found that enhanced-Vs which featured just one of the eleven enhanced-V types had more than a 50% likelihood of being associated with severe weather, and that this percentage increased to greater than 90% when at least six enhanced-V types were present.

ENHANCED-V TYPE	THRESHOLDS NEEDED TO BE MET
A	TMIN < 205 K and TMAX > 213.5 K
B	TMIN < 206 K and TDIFF > 14.5 K
C	TDIFF > 15 K and TMAX > 216 K
D	TMAX > 209 K and DISTARMS > 55 KM
E	TMIN < 201.5 K and DISTARMS > 37.5 KM
F	TDIFF > 16.5 K and DIST < 20 KM
G	TDIFF > 14.5 K and DISTARMS > 59 KM
H	TDIFF > 20 K and ANGLEARMS > 71.5 DEGREES
I	DIST < 18 KM and DISTARMS > 56 KM
J	UL WIND SPD > 50 KT (26 M S^{-1}) and TMIN < 205 K
K	UL WIND SPD > 45 KT (23 M S^{-1}) and TDIFF > 15 K

Table 1: The eleven B06 enhanced-V types and associated threshold criteria. The five types that make no reference to DIST, DISTARMS, or ANGLEARMS are shaded in yellow – see Section 3.

B07's reexamination of the severe weather characteristics of the enhanced-Vs analyzed in their earlier study additionally considered reports of wind gusts ≥ 50 kt (26 m s^{-1}). In a significant revision to their earlier results, they found that the only parameters that had statistically significant severe weather associations were TMIN, TMAX, TDIFF, and UL WIND SPD.

The modified threshold values for these parameters are shown in Table 2. Note that these are very similar to, or identical to the corresponding values defined for the B06 enhanced-V types A, B, C, J and K.

Published studies of Australian severe thunderstorms have almost invariably had a radar and low to mid-level meteorology focus, and have typically been confined to an examination of events, climatologies, and forecast verification in the vicinity of the more populated (mostly capital city) localities (e.g. Buckley et al. 2001, Sills et al. 2004, Schuster and Blong 2004, Deslandes et al. 2007). This paper presents an analysis of eastern Australian severe thunderstorms, based on satellite detection of the enhanced-V signature. The B06/B07 quantitative enhanced-V parameters form a critical component of this analysis. Additionally, this study examines the upper level environments associated with the most intense severe weather outbreaks and enhanced-V signatures.

THRESHOLDS NEEDED TO BE MET
TMIN < 205 K
TMAX > 212 K
TDIFF > 15 K
UL WIND SPD > 50 KT (23 M S^{-1})

Table 2: The modified B07 enhanced-V severe weather thresholds.

2. DATA AND METHODOLOGY

Color-enhanced 1 km resolution 10.8 μm IR NOAA-AVHRR satellite imagery was examined for events of interest over the subtropical eastern Australian mainland (- see Fig. 2 for location of places mentioned in this study). In order to optimize enhanced-V detection and the evaluation of the various B06/B07 quantitative parameters, each satellite scan was examined using a combination of three different enhancements, that cumulatively targeted BT variations between 260 K (-13 °C) and 170 K (-103 °C). Examples of each of these enhancements appear in this paper.

An initial analysis revealed that eastern Australian enhanced-V signatures were far less common than their U.S. counterparts, consistent with the relative severe weather threat experienced in the two countries. So, in order to obtain a sizeable number of enhanced-Vs for analysis, this study examined satellite imagery for 222 eastern Australian severe thunderstorm event days between 1996 and 2007. Furthermore, the selection of days was strongly biased to those associated with (a) major severe weather outbreaks, (b) reports of large hail and/or (far rarer) tornadoes, and (c) warm season occurrences. Additionally, maritime enhanced-Vs detected over the adjacent western Tasman Sea waters on these event days were included in this study.

Details of severe weather occurrences (i.e. hail ≥ 2 cm diameter, wind gusts ≥ 48 kts (89 km h^{-1}), wind damage, and/or tornado sightings) were sourced from the severe weather data bases of the Victorian, New South Wales (NSW), and Queensland Regional Offices of the Bureau of Meteorology (BoM). As in the B07 study, this paper examined the relationship between the enhanced-V and any connected severe weather occurrences within both 0.5 hr and 3.0 hr of the appearance of this signature in the NOAA-AVHRR imagery. For the longer window period, geostationary

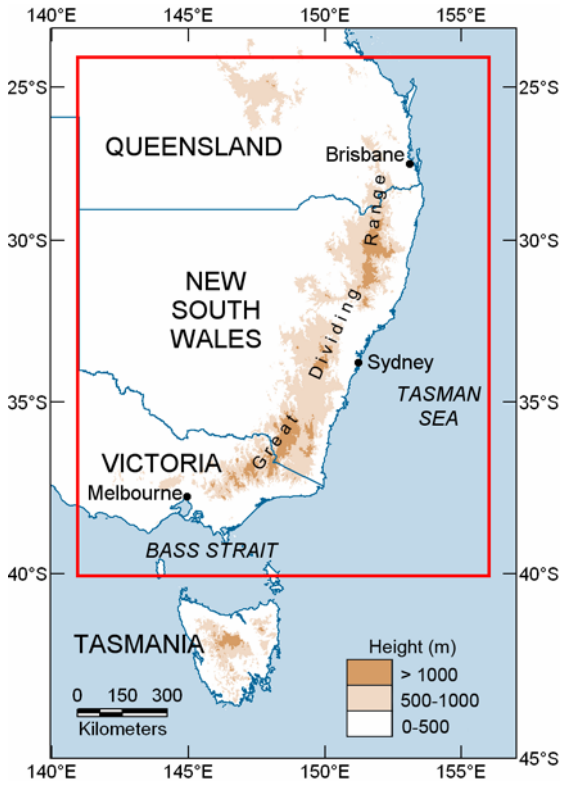

Fig. 2: Location map showing near-coastal topography associated with the Great Dividing Range. Red lines enclose the study area.

satellite imagery (mostly at 1 hourly frequency) from either *GOES-9*, or the Japanese Meteorological Agency's Geostationary Meteorological Satellite (GMS) and Multi-functional Transport Satellite *(MTSAT)-1R* was used to ensure that the enhanced-V signature was present during related severe weather reports more than 1 hr from the time of the NOAA overpass. This study adopted one departure from B07's ± 0.5 hr methodology. B07 attributed all severe weather reports within a 60 km radius of the enhanced-V to that particular feature. Here, BoM archived radar data were used to determine whether or not a particular severe weather event and enhanced-V signature were related.

B07's paper referred to a degree of subjectivity in both the decision to classify a particular satellite imagery feature as an enhanced-V, and in their evaluation of the various enhanced-V parameters, themselves. In their comparative study based on the results of two independent analysts, B07 found the magnitude of the difference in these results to be negligible for the evaluation of TMIN/TMAX/TDIFF, was more significant for values of DISTARMS/ANGLEARMS, and was very large for the DIST parameter. In the latter case, ambiguities principally arose for signatures featuring more than one location with identical values of TMIN and/or TMAX (J. C. Brunner 2008, personal communication). To reduce the extent of this particular problem, this study defined DIST to be the magnitude of the separation of the particular cold and warm features that were nearest each other, thus minimizing the resultant value of DIST. To further address the overall subjectivity concerns, J. C. Brunner assisted in the classification of approximately 60 of the more marginal or complex satellite imagery signatures examined.

A new enhanced-V type with potential meteorological significance was defined in this study – i.e. the TGRAD≥2.0 enhanced-V. These systems were associated with (a) thermal couplet combinations of TDIFF and DIST resulting in a ≥ 2.0 K km^{-1} temperature gradient (TGRAD) between TMIN and TMAX, and (b) TDIFF > 15 K. The system shown in Fig. 1 satisfied these criteria. These conditions were adjusted for a small number of enhanced-Vs that featured more than one prominent cold storm top and/or CWA associated with differing BT values. In such cases, the thermal couplet features chosen to determine TGRAD≥2.0 status were those that contributed to a maximizing of TGRAD, provided that TDIFF remained > 15 K. In all cases, the selected cold or warm entity had BTs within 4 K (and mostly within 2 K) of TMIN or TMAX, respectively. For example, Fig. 3 shows an enhanced-V associated with a well-defined (single) cold storm top,

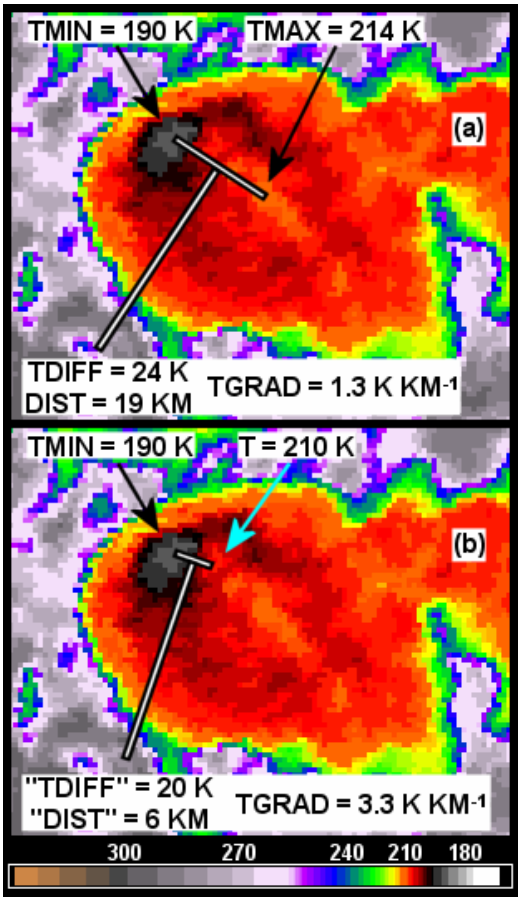

Fig. 3: Enhanced 10.8 μm IR *NOAA-16* AVHRR image valid 0535 UTC 27 November 2005 showing (a) location and values of the B06/B07 thermal couplet parameters and derived TGRAD ((K km^{-1}); and (b) revised CWA parameters defining the TGRAD≥2.0 enhanced-V.

but which displays three discrete downstream enclosed areas of higher BTs within the V arms. The most distant CWA from the storm top was associated with the highest BTs, hence defined TMAX, and determined DIST (Fig. 3a). However, only the nearest (slightly cooler) CWA (see blue arrow in Fig. 3b) contributed to a thermal couplet that easily met the TGRAD≥2.0 enhanced-V definition.

This study also examined the temperature difference between the enhanced-V storm top and the tropopause, including its relationship to severe weather and the various B06/B07 quantitative parameters and enhanced-V types. This temperature difference is subsequently referred to as the Storm Top Temperature Anomaly (STTA; negative values implying overshooting tops). Previous GOES imagery-based studies found a correlation between the STTA magnitude and storm intensity (e.g. Adler et al. 1985), and between the STTA magnitude and TDIFF (Heymsfield and Blackmer 1988). The STTA was also examined because of author concerns about the applicability of the B06/B07 severe weather parameter thresholds to the very different eastern Australian domain.

Except in less than 25% of cases, the resolution of the eastern Australian rawinsonde network was inadequate for evaluating the environmental tropopause temperatures in the vicinity of the detected enhanced-Vs. Instead, these values were sourced from the 250 km resolution NCEP reanalyses (for events prior to March 2004), and the 0-3 hr 100 km resolution GFS Model forecasts (for subsequent events), available from the NOAA National Climatic Data Center (NCDC) web site: (http://www.cdc.noaa.gov/). Tropopause temperatures from these data sets were compared with available rawinsonde data within about 8° latitude/longitude of each enhanced-V, for the 12 hr period encompassing the signature's presence. A discrepancy of ≤ 3 K was observed in nearly 90% of over 500 comparisons, with almost identical results obtained for the two data sets. Of course, a strong relationship should be expected here, given that the rawinsonde data contributed to the NCDC (re)analyses.

The two NCDC data sets were additionally used to determine values of UL WIND SPD, and more general features of the upper tropospheric flow.

High-resolution diagnostics of upper-level divergence were unavailable for this study, so a combination of approaches was used to determine the extent of upper-level forcing in the vicinity of the enhanced-Vs. For events post March 2004, GFS Model divergence diagnostics were used to provide a qualitative indication of forcing associated with broader scale features. Indications of divergence in the upper-level flow were additionally determined from an analysis of BoM archived upper winds, and BoM archived automatically generated Atmospheric Motion Vectors (AMVs). In two events, hour-length Atmospheric Motion Trajectories (AMTs) were manually generated by tracking conservative cold cloud/moisture elements in the *MTSAT-1R* IR and 6.7 μm Water Vapor (WV) imagery. Conventional satellite imagery interpretation techniques for detecting the presence of upper-level forcing were also adopted. Finally, the upper-level environments were compared with those previously diagnosed in U.S. studies to be typically associated with strongly divergent/unbalanced upper-level flow.

3. RESULTS

3.1 Enhanced-V Distribution

The location of enhanced-Vs observed within the study area for the 222 severe thunderstorm event days examined is shown in Fig. 4. There were 146 signatures, associated with 132 different cells. These were concentrated within a 300-400 km wide longitudinal band, which was centered near the central NSW coast, in the south, and 100-200 km inland from the southern Queensland coast, in the north. With the exception of a small region located near the NSW-Queensland border, very few signatures were detected inland from the Great Dividing Range.

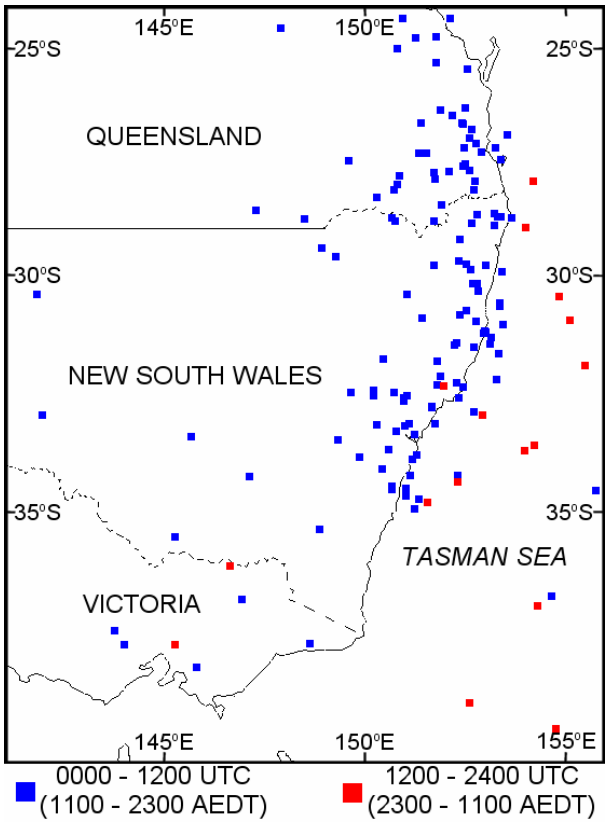

Fig. 4: Map showing location of enhanced-Vs detected within study area. Blue markers indicate enhanced-Vs that occurred between 0000 and 1200 UTC (predominantly afternoon and evening hours), whilst red markers correspond with signatures that occurred between 1200 and 2400 UTC (overnight and morning hours).

It is very likely that maritime cases have been significantly under-represented in this analysis, given that only days associated with mainland severe weather

were examined. It is also possible that this study's bias towards examining major severe weather outbreak days had some impact on the representation of overland enhanced-Vs remotely located from the more populated coastal fringe.

The eastern Australian enhanced-V distribution is largely reflective of the findings of the few published severe weather climatologies of the region, particularly of those pertaining to (large) hail. For example, in their NSW hail climatology, Schuster et al. (2005) observed the highest hail frequencies over coastal and elevated areas near and north of Sydney's latitude, but little hail occurrence further southwards, despite ample storm spotters in this area.

Fig. 4 also shows the dominance of afternoon and evening enhanced-V occurrences, consistent with climatologies on the diurnal frequency of eastern Australian severe weather (e.g. Tucker 2002). However, most of the marine signatures detected well offshore occurred between 1200 and 1900 UTC (i.e. 2300 and 0600 Eastern Daylight (Savings) Time (EDT)).

The monthly distribution of enhanced-V event days and signatures detected for the 222 severe thunderstorm days examined (Fig. 5) also mirrors results from other eastern Australian severe weather studies (e.g. Buckley et al. 2001, Tucker 2002). The spring to early summer months of October to January accounted for 82% and 86% of enhanced-V event days and signatures, respectively. Although enhanced-Vs were most likely to be detected in December (in part, reflecting the large number of severe weather events examined in this month), multiple signatures were far more common for October and January events. No enhanced-Vs were observed during the cool season May-September period.

3.2 Tropopause-Level Winds

An analysis of the tropopause-level winds (not shown) revealed that 126/146 (i.e. 86%) of enhanced-Vs were accompanied by wind strengths between 40 and 65 kt (21 and 33 m s^{-1}), with extremes of 25 kt (13 m s^{-1}) and 100 kt (51 m s^{-1}) observed. These values resemble those of the B06/B07 studies.

3.3 Storm Top Temperature Anomalies

The distribution of STTA values (Fig. 6) indicates that about 80% of signatures had overshooting storm tops > 5 K lower than the environmental tropopause temperature. STTAs between –6 K and –16 K accounted for about two thirds of cases, and an extreme value of –21 K accompanied three signatures. The 11 instances of STTAs ≥ 0 K were either associated with cases where satellite and/or radar data suggested that the enhanced-Vs were weakening, or have been attributed to errors in the tropopause temperature diagnostics.

3.4 Quantitative Enhanced-V Parameter Relationships

Consistent with B07's findings, an initial analysis of DISTARMS and ANGLEARMS also found that these parameters didn't appear to have severe weather associations. The subsequent decision to abandon a detailed examination of the V-arms was also made because it was often difficult to objectively quantify these parameters, particularly for signatures associated with U-shaped arms.

Even after the author's attempt to reduce the subjectivity in evaluating DIST, this parameter (by itself) was not observed to correlate with severe weather events. Accordingly, this study focused mostly on the four parameters that B07 found had severe weather associations – i.e. TMIN, TMAX, TDIFF, and UL WIND SPD. However, these parameters were also examined in the context of their presentation in the initial B06 study (-see types shaded in yellow in Table 1). Thus, a revised group of five B06 enhanced-V types (hereafter

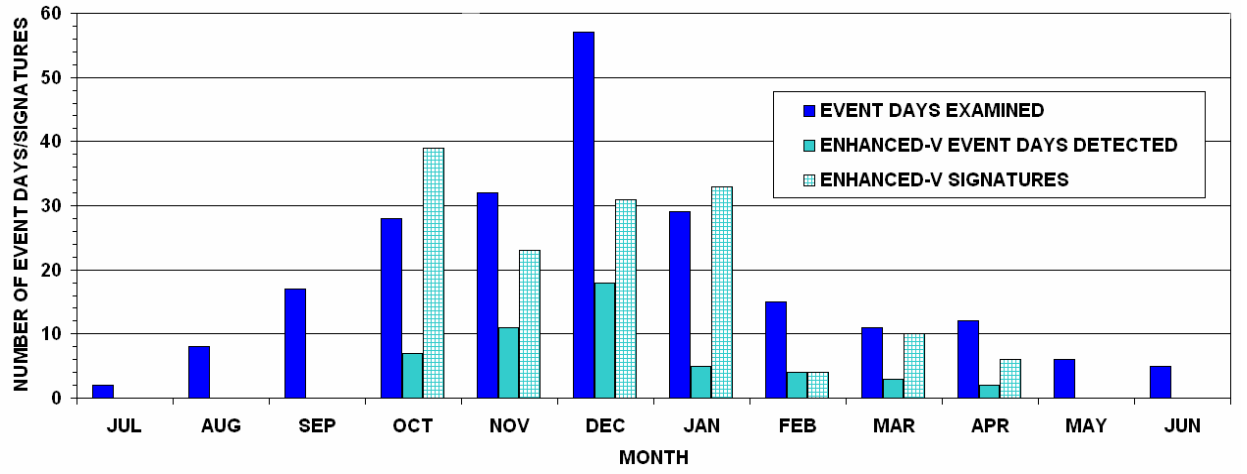

Fig. 5: Monthly frequencies of (severe thunderstorm) event days examined, enhanced-V event days detected, and enhanced-V signatures observed within the study area from 1996-2007.

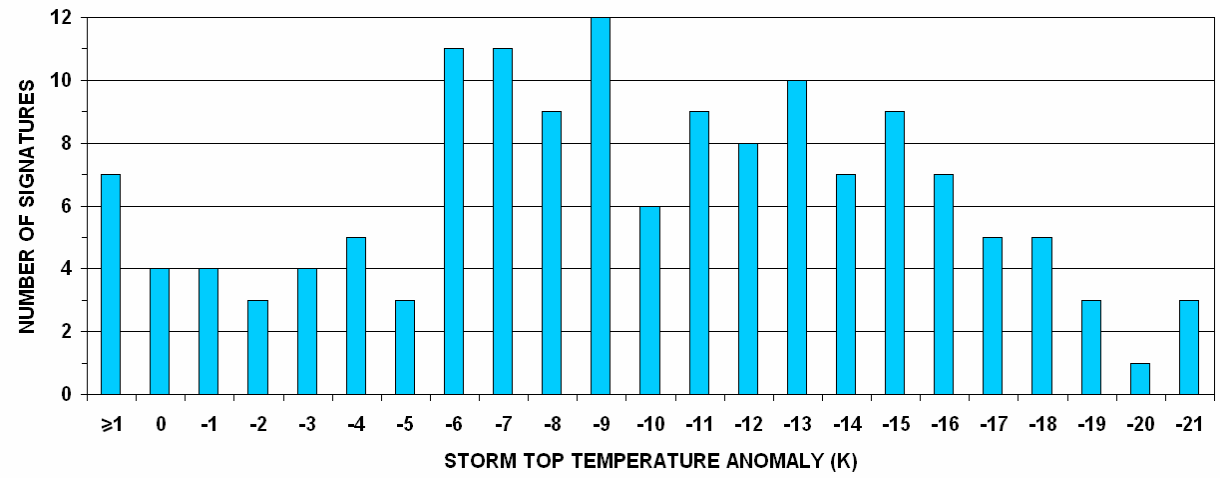

Fig. 6: Distribution of Storm Top Temperature Anomalies (STTAs) (K) for the 146 enhanced-Vs examined.

referred to as revB06 types) was investigated, both for its potential relationship to the STTA, and to eastern Australian severe weather occurrences. In fact, a strong correlation was found between the number of revB06 types present and the magnitude of the storm top overshooting (not shown). Thus, 55 of the 66 (i.e. 86%) signatures characterized by the presence of no more than one revB06 type were associated with STTAs ≥ -10 K, whereas 52 of the 67 (i.e. 78%) signatures that featured at least three of these five types corresponded with STTAs < -10 K.

To help explain these results, the strength of the relationship between the STTA, and the various revB06 types and associated parameter thresholds were analysed (Table 3). Additionally, Table 3 examines the relationship of the STTA to the B07 enhanced-V thresholds, and to the TGRAD≥2.0 enhanced-Vs defined in this paper.

All enhanced-V types/thresholds were found to have significant capability in differentiating between signatures associated with STTAs above and below the study's average/median value of –9.5 K. However, the strongest correlations involved types/parameters that included TDIFF, but excluded TMAX. These are highlighted in yellow in Table 3, whilst the two-dimensional (2D) scatterplot shown in Fig. 7 emphasizes the strong relationship between STTA and TDIFF, particularly for the 90% of signatures associated with STTAs ≤ -2 K.

Finally, only a comparatively small number of signatures met either the B07 or the TGRAD≥2.0 criteria – i.e. 36 and 28 cases, respectively (Table 3).

	ALL	B06 TYPE A	B06 TYPE B	B06 TYPE C	B06 TYPE J	B06 TYPE K	B07	TMIN < 205 K	TDIFF > 16.5 K	UL WIND SPD > 50 KT	TGRAD≥2.0
YES											
NUMBER	146	70	71	49	70	54	36	99	59	90	28
AVE	-9.5	-11.5	-12.9	-11.8	12.2	-13.4	-13.0	-11.5	-13.5	-10.9	-12.5
MED	-9.5	-12.0	-14.0	-13.0	-12.0	-14.0	-14.0	-12.0	-14.0	-11.0	-14.0
NO											
NUMBER	-----	76	75	97	76	92	110	47	87	56	118
AVE	-----	-7.8	-6.4	-8.4	-7.1	-7.3	-8.4	-5.4	-6.9	-7.3	-8.9
MED	-----	-7.5	-7.0	-9.0	-7.0	-7.0	-8.0	-6.0	-7.0	-7.0	-9.0
DIFF											
AVE	-----	3.7	6.5	3.4	5.1	6.1	4.6	6.1	6.6	3.6	3.6
MED	-----	4.5	7.0	4.0	5.0	7.0	6.0	6.0	7.0	4.0	5.0

Table 3: Comparison of average ("AVE") and median ("MED") values of STTA (K) for the 146 enhanced-V signatures that satisfied (i.e. "YES" cases) or failed to meet (i.e. "NO" cases) the B06/B07 thresholds referred to in Tables 1 and 2, and TGRAD≥2.0 enhanced-V thresholds. Also included are the number of signatures assigned to each category, and the difference ("DIFF") in AVE and MED values for the "YES" and "NO" cases in each group. The B06/B07 types/thresholds that include TDIFF and exclude TMAX are highlighted in yellow.

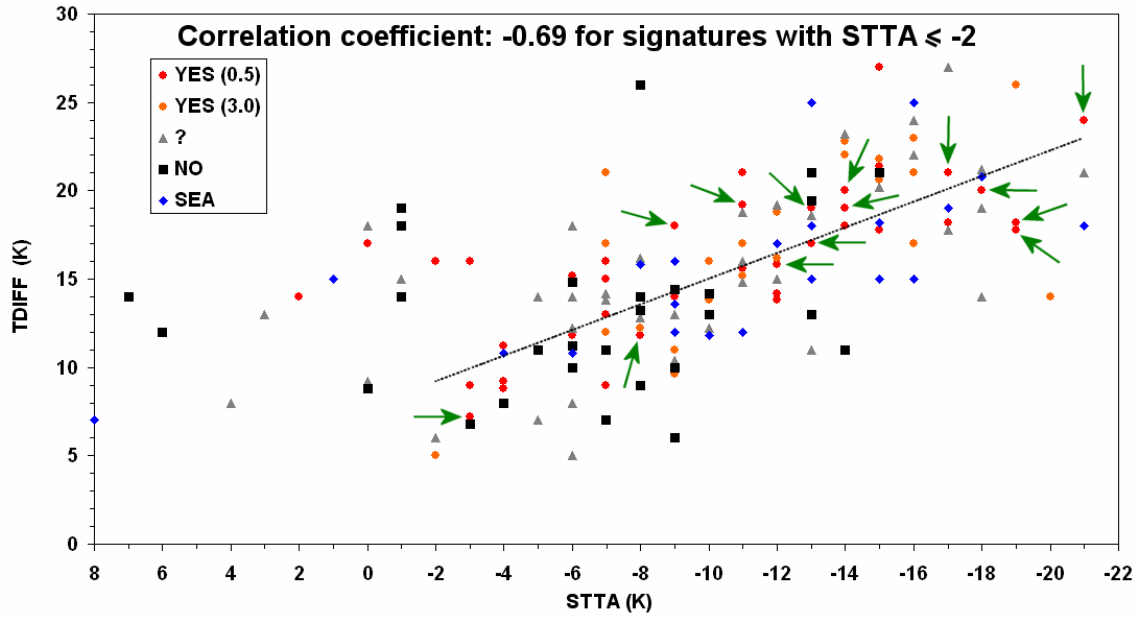

Fig. 7: A 2D scatterplot of STTA (K) and TDIFF (K) for the 146 enhanced-Vs. Each signature has been assigned to one of five categories, according to its severe weather relationship: "YES (0.5)" – severe weather reported within 0.5 hr of the NOAA-AVHRR signature; "YES (3.0)" – severe weather reported with an enhanced-V signature > 0.5 hr but ≤ 3.0 hr from the time of the NOAA-AVHRR signature; "?" – severe weather association unknown; "NO" – no severe weather associated with enhanced-V signature, and "SEA" – maritime signatures. Arrows indicate signatures associated with "high intensity" severe weather – see Section 3.5 text. To avoid overlapping data points, cases with identical values have been slightly displaced along the STTA axis.

3.5 Severe Weather Relationships

This study found that 60/125 (i.e. 48%) of enhanced-Vs characterized by a predominantly overland trajectory had severe weather associations within the ± 3 hr window period, considerably below the 80% value obtained by B07. If the more restrictive ± 0.5 hr window period was applied, a value of 32% was obtained, compared with the corresponding B07 value of 63%. However, radar and satellite data suggest that the relatively low correlation between this study's enhanced-Vs and severe weather episodes was primarily due to the fact that the majority (i.e. 37/65) of the "non-severe" signatures occurred in sparsely populated and remote areas, from which severe weather reports were unlikely to be received. This group included cases where the storm moved through a populated area in a substantially weakened form from the time that the enhanced-V was detected in the NOAA-AVHRR imagery. The limitations of the (eastern) Australian storm spotter network in severe weather analysis and verification have been referred to in several previous studies (e.g. Mills and Colquhoun 1998, Tucker 2002, Schuster et al. 2005).

That not all severe weather reports within a 60 km radius of the enhanced-V were automatically attributed to this feature also contributed to this study's relatively low severe weather association.

A comparison of average values of TMIN, TMAX and TDIFF for the two study regions (Table 4) shows very similar values for these parameters. However, based on the B06/B07 findings, the slightly lower (larger) U.S. values of TMIN (TDIFF) would suggest that these systems had an increased likelihood of severe weather associations. Note that despite the considerably more equatorward mean location of the enhanced-Vs analyzed in the eastern Australian-western Tasman Sea study, Hoinka's (1999) statistical analysis of the global tropopause indicates generally similar values of environmental tropopause temperature for the average U.S. and eastern Australian signatures.

STUDY REGION	LAT.	TMIN	TMAX	TDIFF
U.S. (B06/B07)	38.5 °N	201	217	16
E. AUST – W. TASMAN	30.9 °S	202	217	15

Table 4: Average latitude, TMIN (K), TMAX (K) and TDIFF (K) values for the B06/B07 U.S. and eastern Australian-western Tasman Sea studies. U.S. average latitude provided by J. C. Brunner 2008, personal communication.

The 60 severe weather-producing enhanced-Vs were associated with 50 discrete thunderstorm cells. Of these, 42 (84%) produced large hail, 15 (30%) were associated with non-tornadic strong winds and/or wind damage, and four (8%) spawned tornadoes. The bias

towards examining events associated with large hail and tornadoes is likely to have resulted in an under-representation of non-tornadic wind events in this study.

The significance of the enhanced-V feature to eastern Australian severe weather climatology is emphasized by the fact that within the 1996-2007 study period, this signature was associated with the only two storms that produced hail of ≥ 12 cm diameter, and with the only confirmed warm season tornado of (at least) F2 intensity.

A strong relationship was previously found between the STTA and the number of revB06 types present, principally due to the influence of TDIFF. These three variables were also found to be strong discriminants between severe weather and non-severe weather producing eastern Australian enhanced-Vs, after allowing for the limitations of the storm spotter network.

The 2D scatterplot previously referred to in Fig. 7 also includes the severe weather associations of the enhanced-Vs. Signatures have been classified according to whether they were (a) associated with severe weather within 0.5 hr of the NOAA-AVHRR image (i.e. "YES (0.5)"), (b) associated with severe weather ≤ 3.0 hr but > 0.5 hr from the NOAA-AVHRR image (i.e. "YES (3.0)"), (c) the severe weather association was unknown, due to the absence of reports in a sparsely populated area (i.e. "?"), (d) unassociated with severe weather and traversed a populated area (i.e. "NO"), and marine cases (i.e. "SEA"). Fig. 7 additionally highlights the characteristics of the 14 "YES (0.5)" cases associated with high intensity severe weather (- defined as giant (i.e. ≥ 5 cm diameter) hail, tornadoes of at least F2 intensity, and/or non-tornadic wind gusts ≥ 60 kt (31 m s^{-1})). Most of the "YES (0.5)" and "YES (3.0)" signatures (which in combination are subsequently referred to as "YES (≤ 3.0)" cases) are seen to correspond with highly negative values of STTA, and large values of TDIFF, with the converse relationship holding for the "NO" cases.

A summary of critical values of STTA, TDIFF, and the number of revB06 types present (Table 5) indicates that the transition to systems highly likely to have severe weather associations occurred for enhanced-Vs associated with ≥ 3 revB06 types, for STTAs ≤ –7 to –10 K, and for TDIFFS ≥ 14-16 K. These TDIFF threshold values are essentially identical to those deduced in the B06/B07 studies.

For the case studies presented in Section 4, "strong" enhanced-V signatures have therefore been defined as those that met at least two of the following three criteria: (a) ≥ 3 revB06 types present, (b) TDIFF > 15 K, and (c) STTA ≤ –10 K. The remaining signatures are referred to as "weak". Note that all of the 28 TGRAD≥2.0 enhanced-Vs have consequently been classified as strong systems. Furthermore, of the 16 TGRAD≥2.0 signatures that traversed populated areas within the ± 3.0 hr detection period, 12 had severe weather associations.

Finally, only 27 of the 60 severe weather-associated enhanced-Vs met all of the B07 TMIN, TMAX, and TDIFF thresholds, however seven of these failed to also satisfy the B07 UL WIND SPD threshold. Furthermore, all B07 thresholds were only achieved for five of the fourteen signatures associated with high intensity severe weather. These results suggest that TDIFF/ STTA tended to be relatively stronger discriminants between severe weather and non-severe weather enhanced-Vs for the eastern Australian domain.

CATEGORY	YES (≤ 3.0)	NO	HIGH INTENSITY
revB06 ≥ 3	35/60 (58%)		
revB06 ≤ 1		21/28 (75%)	
revB06 ≥ 3			11/14 (79%)
STTA ≤ -7 K	48/60 (80%)		
STTA > -10 K		23/28 (82%)	
STTA ≤ -8 K			13/14 (93%)
TDIFF ≥ 14 K	46/60 (77%)		
TDIFF < 16 K		22/28 (79%)	
TDIFF ≥ 16 K			12/14 (86%)

Table 5: The ratio (percentage) of "YES ≤ 3.0", "NO", and high intensity severe weather events associated with various threshold values of number of revB06 types, STTA (K) and TDIFF (K).

4. SIGNIFICANT EVENTS

4.1 24 October 2005 - near the north central NSW coast to southeastern Queensland

Eighteen enhanced-Vs were detected in the late afternoon to late evening NOAA imagery for this event, which exceeded the number of these signatures found on any other day examined. They were accompanied by several reports of large hail up to 7.5 cm diameter, and a few reports of wind gusts ≥ 48 kts (89 km h^{-1}).

NOAA-16 IR imagery at 0525 UTC (Figs. 8a and 8b) showed an extensive area of thunderstorms over eastern Australia, within which there were seven enhanced-V signatures. Note that two of the major cells within the southern coastal storm cluster were not categorized as enhanced-Vs at this time, since any attendant V-arms were obscured by the nearby cells. However, they were classified as enhanced-Vs on the subsequent *NOAA-12* image valid 0609 UTC (not shown), whilst a new signature also appeared over southeastern Queensland on the *NOAA-15* image valid 0716 UTC (not shown).

All ten cells featuring enhanced-Vs in the 0525-0716 UTC NOAA imagery developed within diffluent 250 hPa-level flow, downstream of a slow-moving, large scale, negatively-tilted trough (Fig. 8c). The available AMV and rawinsonde data (Fig. 8a)

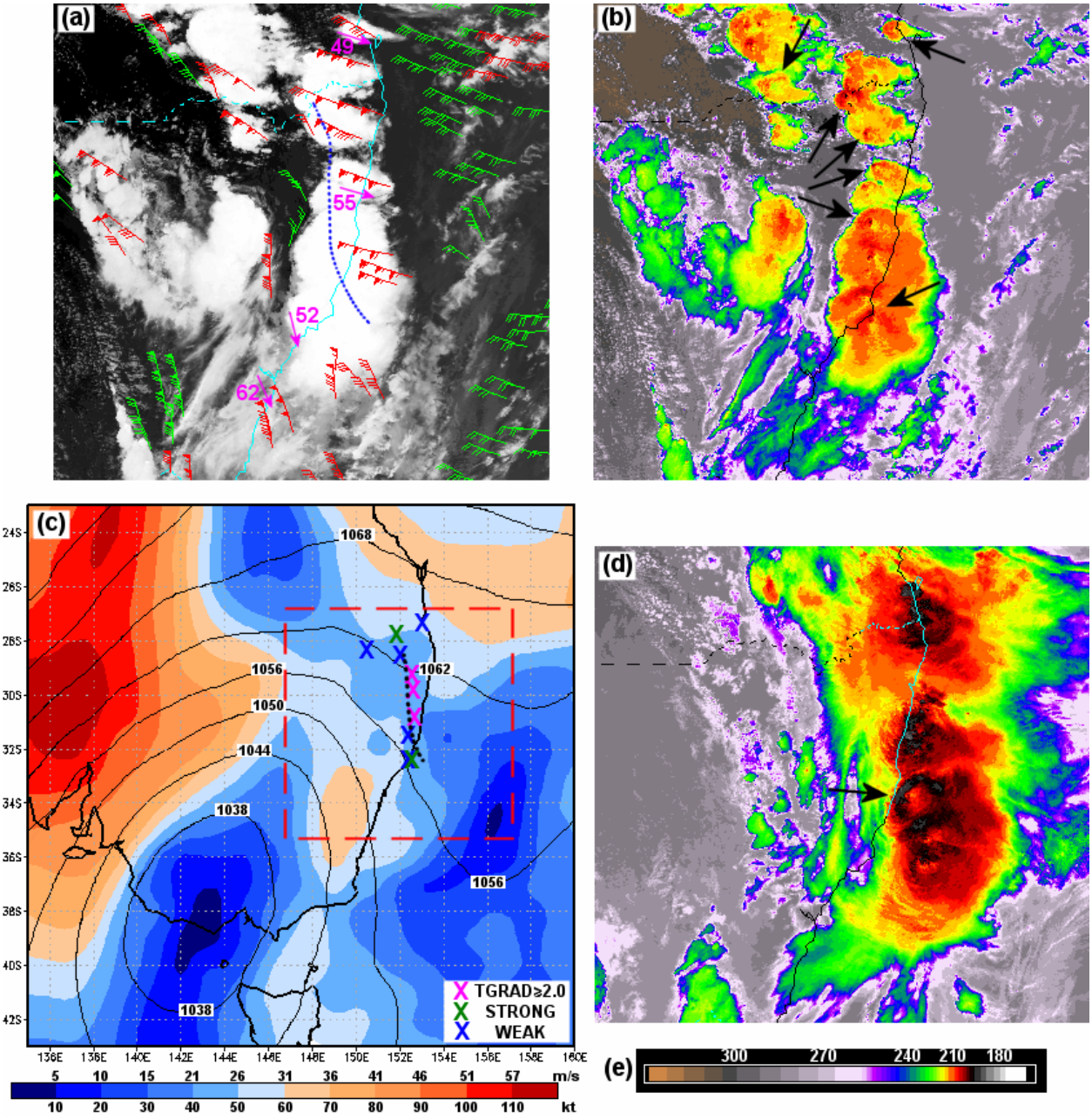

Fig. 8: NOAA-AVHRR satellite imagery and GFS Model upper-air analysis for 24 October 2005: (a) *NOAA-16* unenhanced IR image at 0525 UTC with overlays of 100-400 hPa layer AMVs, and 250 hPa rawinsonde observations (pink arrows show direction, with adjacent plots of speed (kt)). For clarity, AMV data shown in green and red color combination. Dotted blue line defines axis of strong diffluence; (b) corresponding color-enhanced image with arrows indicating location of enhanced-V signatures; (c) 250 hPa analysis at 0600 UTC of geopotential height (solid lines, 60 dam intervals) and isotachs at 10 kt intervals, as in color scale. Dashed red lines show domain of satellite imagery. Crosses denote locations of ten discrete enhanced-V cells detected from NOAA imagery at 0525 UTC, 0609 UTC, and 0716 UTC. Associated colors indicate enhanced-V intensity, as per legend. Dotted black line as for blue dotted line in (a); (d) *NOAA-14* enhanced IR image at 1100 UTC, with arrow indicating enhanced-V signature; and (e) BT scale (K) for enhancements (b) and (d).

additionally showed that within this area of broadscale diffluence, there was a concentrated zone of enhanced diffluence/divergence (denoted by the blue dotted line), across which the winds shifted sharply from a nearly northerly orientation, to one that was from the west-northwest. GFS Model upper-level diagnostics valid

0600 UTC (not shown) indicated that this zone largely coincided with strong values of divergence (i.e. up to 9 X 10^{-5} s^{-1}), and values of absolute vorticity between –6 and +3 X 10^{-5} s^{-1}, indicative of probable inertial instability (e.g. Blanchard 1998, Staudenmaier, 2003). Most of the ten cells were sited in this region of enhanced upper level forcing (Fig. 8c), including the five strong signatures, all of which were associated with STTAs between –11 K and -16 K. Three of these additionally met the TGRAD≥2.0 thresholds (Fig. 8b), one of which was previously presented in Fig. 1.

By 1100 UTC, the main area of convection had consolidated near the east coast, whilst there had been a significant cooling and expansion of the cold storm tops (Fig 8d). The event's fourth TGRAD≥2.0 enhanced-V, characterized by an STTA of –15 K, was located just off the mid-north NSW coast at this time. The cell immediately to its north, which featured a prominent enhanced-V signature in the *MTSAT-1R* imagery at 0950 UTC (not shown), had an STTA of –21 K. This equaled the most extreme value detected for enhanced-Vs in this study. GFS Model output and verifying upper-air rawinsonde observations (not shown) indicated that the 70 kt (36 m s^{-1}) jet streak previously located over southeastern NSW at 0600 UTC (Fig. 8c) had moved to the central NSW coast and intensified to > 100 kt (51 m s^{-1}) by this time. Accordingly, the two intense storm signatures evident at 1100 UTC formed in a region of strong downstream acceleration in the upper-level winds, resulting in coincident GFS Model divergences in the 200-300 hPa layer as large as 30 X 10^{-5} s^{-1}.

4.2 27 November 2005 - southeastern Queensland

This event was associated with the rare F2 tornado which affected the northern outskirts of Brisbane. The *NOAA-16* image valid just after the tornado struck (Fig. 9a) showed a pair of enhanced-Vs in the vicinity of Queensland's capital city, the northernmost of which accompanied the tornado. Both of these signatures were also associated with reports of large hail up to 5 cm diameter. Two additional enhanced-Vs further to the northwest had no severe weather associations, however they were passing through sparsely populated terrain at this time.

All four signatures met the TGRAD≥2.0 enhanced-V criteria, the only such example found within a confined area for any event analysed. The accompanying STTAs ranged between –11 K and –16 K.

This event appears to have been associated with a narrow zone of intense upper-level diffluence/ divergence (emphasized by the dotted lines in Figs. 9a and 9b) analogous to that detected in the previous case study. Thus, the anvil-level flow was directed towards the east-northeast for the three easternmost enhanced-Vs, and to the southeast for the remaining signature, and for other cells further to the northwest. Since the anvil orientation tends to be indicative of the storm relative flow, rather than the actual upper-level wind flow (e.g. Heymsfield and Blackmer 1988), it cannot be automatically assumed that the upper level winds were necessarily strongly diffluent in this region. However, this was not an issue for this event, since there was minimal difference in the storm motion of these relatively slow-propagating cells. Consequently, the anvil-level flow along the southern Queensland coast had an identical orientation to Brisbane's 0600 UTC 200 hPa wind (Fig. 9b).

The GFS Model 200 hPa-level geopotential height and isotach analysis (Fig. 9b) included a rapidly amplifying trough, and a downstream 90 kt (46 m s^{-1}) jet streak located just to the south of the enhanced-Vs. The jet streak was propagating into a short-wave ridge, which is a scenario that has often been found to be associated with strongly unbalanced flow (e.g. Uccellini et al. 1984, Bluestein and Thomas 1984). In this event, winds crossing the geopotential height contours at angles of as much as 60-70 degrees were indicative of the presence of strongly ageostrophic upper-level flow extending from the southern Queensland coast to the central NSW coast (Fig. 9b). GFS Model 200 hPa divergences of up to 8 X 10^{-5} s^{-1} were diagnosed in the vicinity of the enhanced-Vs (Fig. 9c), with coincident values of absolute vorticity (not shown) suggesting the likely presence of inertial instability.

4.3 25 October 2003 - eastern Queensland-NSW border region

One of the most intense severe weather outbreaks ever recorded over subtropical eastern Australia occurred on this day, but this case study focuses only on a limited region impacted. Enhanced NOAA imagery during the early evening showed extensive thunder-storm activity over southeastern Queensland and northern NSW, including the presence of two strong enhanced-Vs (Fig. 10a). STTAs of –16 K and –19 K were associated with the western and eastern signatures, respectively. However, these cells mostly traversed remote, sparsely populated terrain, resulting in just one severe weather report of 5 cm diameter hail with the eastern feature.

An analysis of the anvil-level flow (Fig. 10a), together with available AMV data (not shown), suggested the presence of strong diffluence in the vicinity of the two enhanced-Vs at this time. GFS Model diagnostics of upper-level forcing were not available for this event. However, the synoptic setting (not shown) was one that previous studies had found to be highly conducive to the development of strongly divergent upper-level flow near a short wave ridge (e.g. Uccellini et al. 1984, Zack and Kaplan 1987, Moore and Abeling 1988). Thus, for this case a highly mobile, negatively tilted trough in the exit region of an approximately 110 kt (57 m s^{-1}) 250 hPa jet streak approached a slow-moving, amplifying short wave ridge. The AMV data indicated that the enhanced-Vs were located near, but on alternative sides of this ridge.

Closer examination of the eastern enhanced-V using a different enhancement (Fig. 10b) revealed that this signature did not merely achieve TGRAD≥2.0 status, but was associated with the most intense thermal couplet temperature gradient detected in this study. Thus, BTs

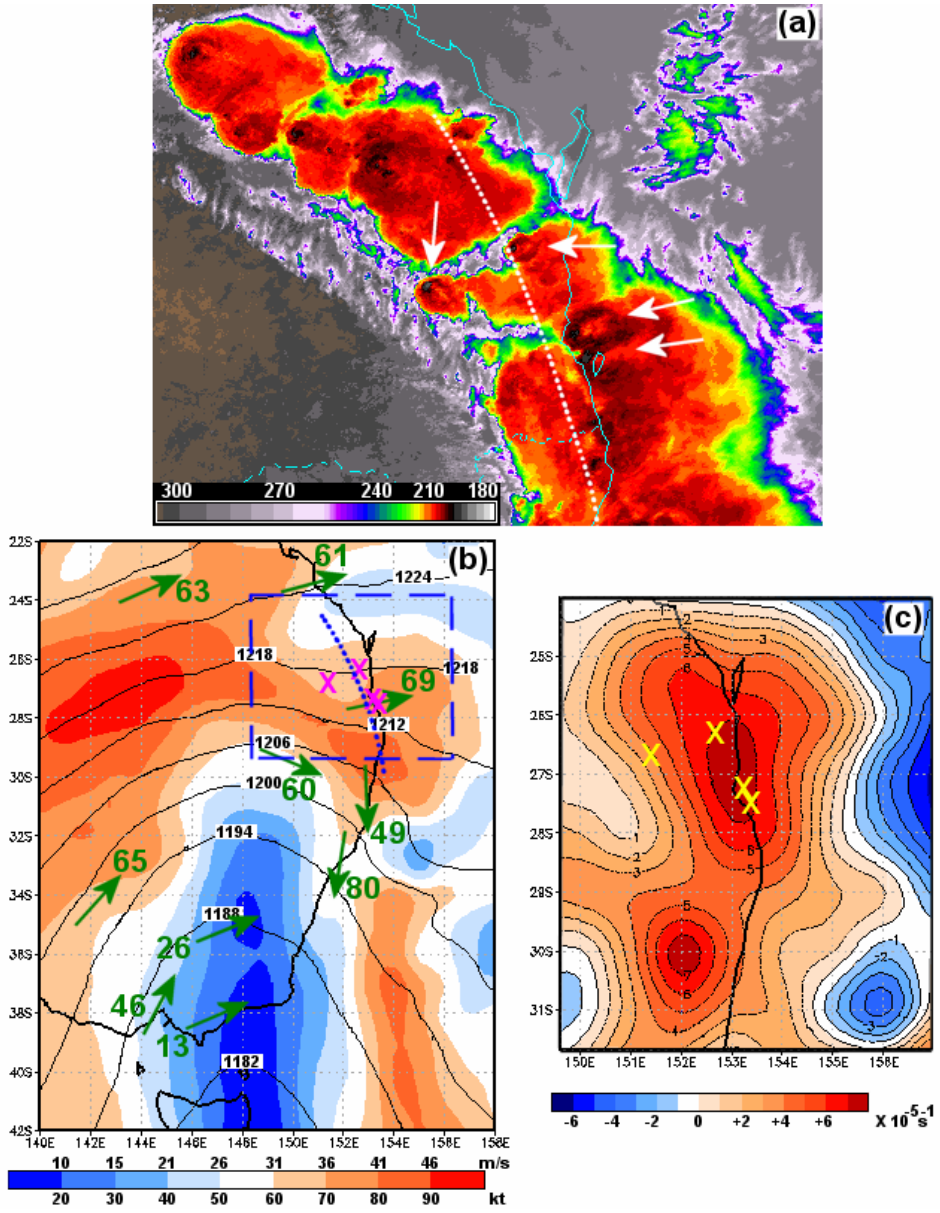

Fig. 9: NOAA-AVHRR satellite image and GFS Model 200 hPa analyses for 27 November 2005: (a) *NOAA-16* enhanced IR image at 0535 UTC. Arrows show location of enhanced-Vs. Dotted line denotes axis of strong directional shift in anvil-level airflow; (b) 0600 UTC analysis of geopotential height (dam) and isotachs (kt) - conventions as in Fig. 8c. Verifying rawinsonde wind observations shown in green: arrows indicate direction, with adjacent plots of speed (kt). Dotted line as in (a). Dashed lines show domain of satellite image; and (c) 0600 UTC analysis of divergence (X 10^{-5} s^{-1}). Crosses show location of enhanced-Vs.

of 197 K and 222 K for the storm top and the nearest CWA, respectively, combined with a separation of just 4 km, resulted in an associated TGRAD of 6.3 K km^{-1}. Note that this signature was associated with more than one prominent CWA, with a TMAX of 223 K actually occurring with the more distant CWA. The resultant TDIFF of 26 K was just 1 K less than the maximum value observed for this parameter in this study. In comparison, the B06/B07 studies analyzed an extreme TDIFF value of 41 K. Fig. 10b also reveals that the two CWAs were separated by a transverse band of considerably lower BTs that extended between the two V-arms. In fact, the enhancements show a sequence of wave-like thermal perturbations extending downstream from TMIN. The 2D configuration of this downstream thermal wave (Fig. 10c) indicates that the waves were situated near the tropopause, and characterized by a 10-12 km wavelength that rapidly decreased in amplitude downstream. The appearance of this feature is consistent with the Heymsfield et al. (1983) and Lin

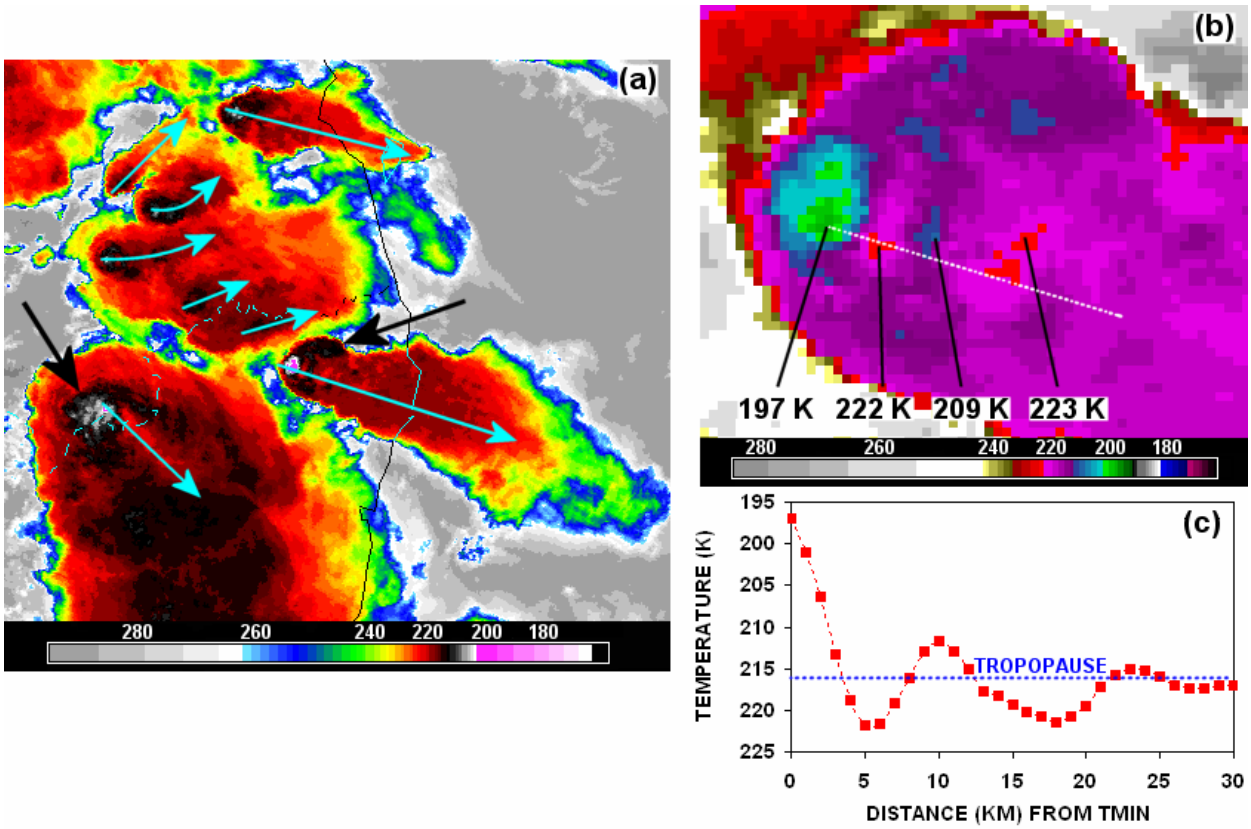

Fig. 10: (a) and (b): *NOAA-12* enhanced IR imagery at 0702 UTC 25 October 2003. Black arrows in (a) show location of two enhanced-Vs, and blue arrows show the direction of the anvil-level flow. Magnified, different color enhancement of easternmost enhanced-V shown in (b), including BTs (K) of cold storm top (TMIN) and downstream features. White dotted line defines location of 30 km-length cross-section shown in (c); (c) graph showing BT (K) variation downstream from TMIN, and its relationship to the tropopause temperature on the corresponding 0600 UTC NCEP reanalysis. BT values at data points downstream from TMIN averaged over a 2 km length.

(1986) studies which proposed that CWAs are generated by wave-induced subsidence downwind of the storm top. Thermal waves were noticed with 10 of the 146 enhanced-Vs examined, including the TGRAD≥2.0 enhanced-V shown in Fig. 3. Most were associated with STTAs ≤ -15 K.

4.4 7 December 2005 - centered over northeastern Victoria

Several factors contributed to make this an exceptional event. An outbreak of thunderstorms over the eastern half of Victoria and adjacent parts of southern NSW occurred during the early morning (Fig. 11a). This was accompanied by four reports of large hail, including a report of 5 cm diameter hail with an enhanced-V system (position indicated with black arrow). Severe thunderstorm climatologies (e.g. Tucker 2002) indicate that early morning large hail episodes are extremely rare over eastern Australia, and this was the only example of an early morning giant hail occurrence within the Victorian-NSW region for the 1996-2007 period examined.

A detailed analysis of Victorian radar data (not shown) revealed that this event was characterized by a 5-hour period in which there were in excess of 20 cells that featured elevated, high (i.e. ≥ 50 dBz) reflectivity cores comparable to those associated with the large hail reports. Most of these traversed remote, alpine terrain in eastern Victoria. Additionally, the 50 dBz reflectivity core for the cell associated with the enhanced-V attained elevations almost 2 km higher than those achieved prior to the 5 cm hail report. This strongly suggests that this cell was capable of producing hail of even greater size.

Only seven enhanced-Vs were observed within Victoria over the 84 severe thunderstorms event days examined for this State (Fig. 4). The system for this event was one of only two strong signatures detected in Victoria. It featured all five revB06 types, a TDIFF of 18 K, and an STTA of –9 K.

Severe weather developed ahead of a comma cloud associated with mid to upper-level cyclogenesis (see dotted lines on cirriform cloud bands in Fig. 11a). Approximately an hour later, this system appeared in the GFS Model 250 hPa-level flow (Fig. 11b) as a (highly mobile) negatively-tilted short wave trough located in the exit region of an approximately 120 kt

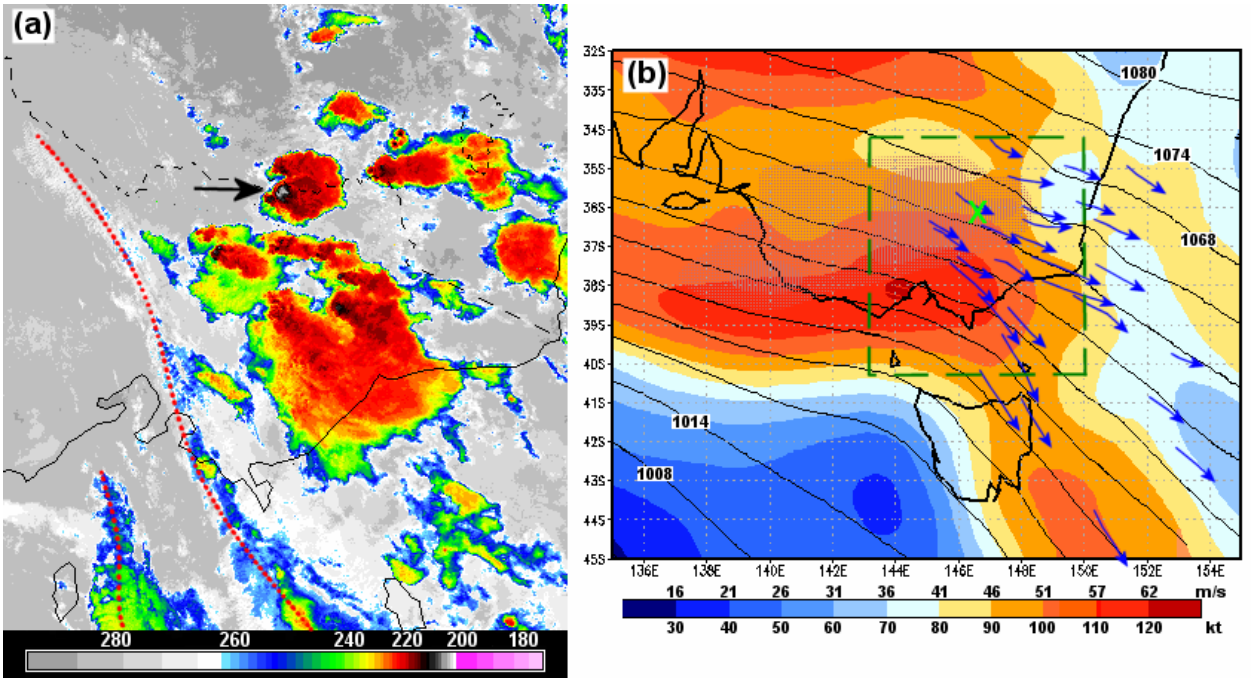

Fig. 11: (a) *NOAA-16* enhanced IR image at 1653 UTC 6 December 2005 (0353 EDT 7 December). Arrow indicates location of enhanced-V. Dotted lines denote axis of all but southernmost section of upstream comma cloud feature; and (b) corresponding GFS Model 250 hPa analysis at 1800 UTC of isotachs (kt) and geopotential height (dam). Conventions as in Fig. 8c. Stippled (vertical line) areas associated with absolute vorticity values ≥ -6 and < -3 X 10^{-5} s^{-1} (≥ -3 X 10^{-5} s^{-1}). Hour-length AMTs (blue arrows) based on 1750-1850 UTC *MTSAT-1R* IR and 6.7 μm WV imagery, and mostly correspond to the 200-400 hPa layer. Cross shows location of enhanced-V. Dashed lines outline domain of satellite imagery.

(62 m s^{-1}) jet streak that was approaching a (slow-moving) short wave ridge. The ridge was located just inland from the southern NSW coast. This scenario was analogous to that described in the previous case study, and which was shown to be commonly associated with strongly divergent upper-level flow. The enhanced-V additionally formed in a region of low inertial stability (- indicated by vertical line shading in Fig. 11b), within the anticyclonic exit region of the jetstreak

Fig. 11b also includes a manual analysis of the hour-length AMTs obtained from the *MTSAT-1R* IR and 6.7 μm WV imagery over four time steps from 1750-1850 UTC (blue arrows). These primarily corresponded with features associated with BTs for the 200-400 hPa layer. The AMTs indicate that highly diffluent upper-level flow existed ahead of the short wave trough, consistent with the characteristics of the anvil level flow shown in Fig. 11a. Furthermore, they show that there was marked speed divergence downstream from the vicinity of the enhanced-V feature. That is, the AMTs over north-eastern Victoria and adjacent parts of NSW were generally characterized by (hour-averaged) speeds of 70-80 kt (36-41 m s^{-1}), whist several of the AMTs located in the vicinity of eastern Bass Strait were associated with speeds of 100-125 kt (51-64 ms^{-1}). The presence of strong upper-level forcing and unbalanced flow in the severe weather area was further implied by several AMTs within the jet streak exit zone that were directed towards lower geopotential heights.

5. CONCLUSIONS AND DISCUSSION

This study analysed the characteristics of 146 enhanced-Vs detected in NOAA-AVHRR imagery for the eastern Australian-western Tasman Sea region. Despite the considerably lower frequency of eastern Australian-western Tasman Sea enhanced-Vs, they were found to have characteristics that were generally very similar to those studied by B06/B07. Additionally, they developed in tropopause-level flow of similar strength. Adopting a similar ± 3.0 h (± 0.5 h) window detection methodology to that used by B07, this study found that 48% (32%) of the overland signatures were associated with severe weather reports, which were significantly lower percentages than those deduced by B06/B07. This difference was primarily attributed to the fact that the majority of the eastern Australian enhanced-Vs without severe weather associations occurred in sparsely populated and remote areas, from which severe weather reports were unlikely to be received.

The geographical distribution of enhanced-Vs was consistent with previous climatologies of severe thunderstorm distribution within the eastern Australian region. The relevance of the enhanced-V to severe

weather in this region was reinforced by the fact that these signatures typically featured in the most intense severe weather events detected during the 1996-2007 study period.

After allowing for the deficiencies in the storm spotter network, TDIFF was found to be the strongest discriminant between severe weather and non-severe weather signatures. This B06/B07 quantitative parameter was found to correlate strongly with the magnitude of the STTA, consistent with Heymsfield and Blackmer's (1988) results obtained using lower resolution GOES imagery.

As with the B06/B07 studies, an enhanced-V with a TDIFF > 15 K was observed to have a high likelihood of severe weather associations. This corresponded with an STTA approximately < -10 K. In comparison with the B06/B07 studies, threshold values of TMIN, TMAX, and UL WIND SPD appeared to be less important in determining severe weather potential for the eastern Australian enhanced-Vs. However, ideally a larger number of severe weather signatures would need to be examined in order to confirm these results.

Case studies of four significant weather events demonstrated that these all occurred in environments characterized by pronounced upper-level forcing. These findings were additionally found to be representative of other significant events not included in this paper. In summary, strong upper-level forcing was observed with the largest hail events, and with the sole warm season F2 tornado. It was also observed with the longest lasting enhanced-Vs, and with systems that featured the largest values of TDIFF, and the most negative values of STTA. Most notably, strong upper forcing was prominent in the vicinity of all 28 TGRAD≥2.0 enhanced-Vs detected.

That inertial instability very likely featured in at least three of the four presented case studies, including those associated with the rare F2 tornado and an exceptional nocturnal giant hail development, was particularly noteworthy. Staudenmaier's (2003) paper on severe weather associated with the North American Monsoon referred to the tendency for convective systems to grow upscale overnight in areas of inertial instability. Additionally, Thompson and Edwards (2000) diagnosed likely inertial instability in the vicinity of the Oklahoma-Kansas tornado outbreak of 3 May 1999. These two papers both referred to research by Blanchard et al. (1998) that hypothesized that the equilibrium-level convective outflow is unconstrained in regions of inertial instability, resulting in enhanced storm-top divergence. The findings of this eastern Australian-western Tasman Sea study give greater weight to the likely important role played by inertial instability in severe thunderstorm developments.

The observation that the most intense severe weather within the eastern Australian-western Tasman Sea generally occurred in environments associated with strong upper-level forcing is consistent with U.S.-based severe weather research (e.g. Rogash and Racy 2002, Boustead and Schumacher 2006, Britt and Glass 2006). The BoM's operational National Thunderstorm Forecast Guidance System (NTFGS; Hanstrum 2003) uses algorithms based essentially on characteristics of the low to mid-tropospheric meteorology to diagnose environments favorable for a variety of convective phenomena within the Australian region. The results of this study, consistent with those of the U.S.-based studies, suggest that NTFGS should be modified to include diagnostics of upper-level forcing, in order to enhance its ability to provide quality guidance of (severe) thunderstorm threat areas to forecasters.

Acknowledgements. The author expresses his deep gratitude to Jason Brunner for his encouragement and support of this research, including his invaluable assistance in the classification of many of the satellite imagery signatures examined. This paper also benefited from reviews provided by Michael Reeder and Harvey Stern. Access to archived Bureau of Meteorology atmospheric motion vector data was provided by John Le Marshall and Rolf Seecamp. Tony Wedd is thanked for his considerable efforts in providing the author with additional details on Queensland severe weather events.

REFERENCES

Adler, R. F., and R. A. Mack, 1986: Thunderstorm cloud top dynamics as inferred from satellite observations and a cloud top parcel model. *J. Atmos. Sci*., **43**, 1945-1960.

____, M. J. Markus, and D. D. Fenn, 1985: Detection of severe Midwest thunderstorms using geosynchronous satellite data. *Mon. Wea. Rev.*, **113**, 769-781.

____, ____, ____, G. Szejwach, and W. E. Shenk, 1983: Thunderstorm top structure observed by aircraft overflights with an infrared radiometer. *J. Appl. Meteor*., **22**, 579-593.

Blanchard, D. O., W. R. Cotton, and J. M. Brown, 1998: Mesoscale circulation growth under conditions of weak inertial stability. *Mon. Wea. Rev*., **126**, 118-140.

Bluestein, H. B., and K. W. Thomas, 1984: Diagnosis of a jet streak in the vicinity of a severe weather outbreak in the Texas Panhandle. *Mon. Wea. Rev.*, **112**, 2499-2520.

Boustead, J. M., and P. N. Schumacher, 2006: Synoptic evolution of significant tornado days over Nebraska and Iowa from the spring through mid summer. Preprints, 23rd *Conf. Severe Local Storms*, St. Louis, MO, Amer. Meteor. Soc. [CD-ROM].

Britt, M. F., and F. H. Glass, 2006: Environmental and synoptic conditions associated with cool season strong and violent tornadoes in the north central United States. Preprints, 23rd *Conf. Severe Local Storms*, St. Louis, MO, Amer. Meteor. Soc. [CD-ROM].

Brunner, J. C., S. A. Ackerman, A. S. Bachmeier, and R. M. Rabin, 2006: A quantitative analysis of the

enhanced-V signature in relation to severe weather. Preprints, *Symposium on the Challenges of Severe Convective Storms*, Atlanta, GA, Amer. Meteor. Soc. [CD-ROM].

____, ____, ____, and ____, 2007: A quantitative analysis of the enhanced-V signature in relation to severe weather. *Wea. Forecasting*, **22**, 853-872.

Buckley, B. W., L. M. Leslie, and Y. Wang, 2001: The Sydney hailstorm of April 14, 1999: Synoptic description and numerical simulation. *Meteorol. Atmos. Phys*., **76**, 167-182

Deslandes, R. B., A. J. Bannister, and H. Richter, 2007: The end to end severe thunderstorm forecasting system in Australia: Overview and training issues. *33rd International Conf. Radar Meteorology*, Cairns, Australia, Amer. Meteor. Soc.

Hanstrum, B. N., 2003: A National NWP-based thunderstorm and severe thunderstorm forecasting guidance system. 15th Annual Workshop of Meteorology Research Centre (BMRC) Modelling Workshop: 'Current issues in the paramerization of convection' October 13th to October 16th, 2003. Extended abstracts, Bureau of Meteorology Research Centre, Melbourne.

Heymsfield, G. M., and R. H. Blackmer Jr., 1988: Satellite-observed characteristics of Midwest severe thunderstorm anvils. *Mon. Wea.* Rev., **116**, 2200-2224.

____, ____, and S. Schotz, 1983: Upper-level structure of Oklahoma tornadic storms on 2 May 1979. I: Radar and satellite observations. *J. Atmos. Sci.*, **40**, 1740-1755.

Hoinka, K. P., 1999: Temperature, humidity, and wind at the global tropopause. *Mon. Wea. Rev.*, **127**, 2248-2265.

Lin, Y.–L., 1986: Calculation of airflow over an isolated heat source with application to the dynamics of V-shaped clouds. *J. Atmos. Sci.*, **45**, 2987-3002.

McCann, D. W., 1983: The enhanced-V: A satellite observable severe storm signature. *Mon. Wea. Rev.*, **111**, 887-894.

Mills, G. A., and J. R. Colquhoun, 1998: Objective prediction of severe thunderstorm environments: Preliminary results linking a decision tree with an operational regional NWP model. *Wea. Forecasting*, **13**, 1078-1092.

Moore, J. T., and W. A. Abeling, 1988: A diagnosis of unbalanced flow in upper levels during the AVE-SESAME I period. *Mon. Wea. Rev*., **116**, 2425-2436.

Rogash, J. A., and J. Racy, 2002: Some meteorological characteristics of significant tornado events occurring in proximity to flash flooding. *Wea. Forecasting*, **17**, 155-159.

Schlesinger, R. E., 1984: Mature thunderstorm cloud-top structure and dynamics: A three-dimensional numerical simulation study. *J. Atmos. Sci.*, **41**, 1551-1570.

Schuster. S. S., and R .B. Blong, 2004: Hailstorms and the estimation of their impact on residential buildings using radar. Preprints, 6th International Symposium on Hydrological Applications of Weather Radar. Melbourne, Australia, 2-4 February, 2004.

____, ____, and M. S. Speer, 2005: A hail climatology of the greater Sydney area and New South Wales, Australia. *Int. J. Climatol.*, **25**, 1633-1650.

Sills, D. M. L., J. W. Wilson, P. I. Joe, D. W. Burgess, R. M. Webb, and N. I. Fox, 2004: The 3 November tornadic event during Sydney 2000: Storm evolution and the role of low-level boundaries. *Wea. Forecasting*, **19**, 22-42.

Staudenmaier, M. Jr., 2003: A WES examination of the environment of the 10-11 September 2002 severe weather outbreak. Western Region Technical Attachment No. 03-32.

Thompson, R. L., and R. Edwards, 2000: An overview of environmental conditions and forecast implications of the 3 May 1999 tornado outbreak. *Wea. Forecasting*, **15**, 682-699.

Tucker, D. F., 2002: Characteristics of severe hail events in eastern Australia. Preprints, *21st Conf. on Severe Local Storms*, San Antonio, TX, Amer. Meteor. Soc. pp. 91-94.

Uccellini, L. W., P. J. Kocin, R. A. Petersen, C. H. Wash, and K. F. Brill, 1984: The Presidents' Day cyclone of 18-19 February 1979: Synoptic overview and analysis of the subtropical jet streak influencing the pre-cyclogenetic period. *Mon. Wea. Rev.*, **112**, 31-55.

Zack, J. W., and M. L. Kaplan, 1987: Numerical simulations of the subsynoptic features associated with the AVE-SESAME I case. Part I: The preconvective environment. *Mon. Wea. Rev*., **115**, 2367-2394.